

Development of Scale Invariant Physically Based Hydrological Model: Scale Invariant TOPMODEL

Nawa Raj PRADHAN*, Yasuto TACHIKAWA and Kaoru TAKARA

*Graduate School of Civil Engineering, Kyoto University

Synopsis

Higher resolution topographic information contained in the topographic index of TOPMODEL is lost when a coarse grid resolution DEMs are used. This research has introduced a resolution factor and a fractal method for scaled steepest slope in the topographic index to account for the scale effect in up-slope contributing area per unit contour length and slopes respectively. The method being successful to derive a topographic index distribution of a fine resolution DEM by using only coarse resolution DEM, has been coupled with TOPMODEL to develop Scale Invariant TOPMODEL. The simulated runoff from the Scale Invariant TOPMODEL applied at 1000m grid resolution DEM of Kamishiiba catchment (210 km²) in Japan, with the same set of effective parameter values derived from 50m grid resolution DEM, have matched with the simulated runoff of the 50m DEM resolution TOPMODEL.

Keywords: scale invariant, downscale, fractal method, topographic index distribution, TOPMODEL

1. Introduction

Despite the enormous capacity of today's (and tomorrow's) information technologies, the complexity of the Earth's surface is such that the most voluminous descriptions are still only coarse generalizations of what is actually present (Goodchild, 2001). This implies that the need for continued and sustained research on scale issues is therefore self-evident. In the field of hydrology, since

the introduction of the first blueprint of a distributed hydrological model (Freeze and Harlan, 1969) the desire to develop more physically realistic distributed models has been motivated for forecasting changes in hydrological behavior due to a variety of land use and climate changes and for hydrologic predictions in ungauged basins. An important part of this goal is to replace the dependence of models on calibrated 'effective parameters' with physically realistic process descriptions that use parameters inferred from

the direct observation of land surface conditions.

As the spatial extent is expanded beyond point experiments to larger watershed regions, the direct extension of the point models requires an estimation of the distribution of model parameters and process computations over the heterogeneous land surface. If a distribution of a set of spatial variables required for a given hydrological model (e.g. surface slope, soil hydraulic conductivity) can be described by a joint density function, then digital elevation models (DEMs) and geographical information systems (GISs) may be evaluated as a tool for estimating this function. Now the question to be asked is whether current GISs and current available spatial data sets are sufficient to adequately estimate these density functions.

Several researches (Quinn *et al.*, 1991; Wolock and Price, 1994; Zhang and Montgomery, 1994; Iorgulescu and Jordan, 1994; Bruneau *et al.*, 1995; Fran chini *et al.*, 1996; Saulnier *et al.*, 1997; Mendicino and Sole, 1997) have discussed the effects of digital elevation model map scale and data resolution on the distribution of the topographic index, concluding that there is interdependence between DEM scale and topographic index distribution. Lack of a method for the translation of the scale dependence relations into effective hydrological models have posed a serious problem for the ungauged basins of developing countries where only coarse resolution DEM data, e.g. 30 arc second resolution DEM data set in GTOPO30, USGS web site, is available (Pradhan and Jha, 2003).

Band and Moore (1995) point out that higher frequency topographic information is lost as the larger sampling dimensions of the grids act as filter. This is one of the nature and extent of the scale problem and without a method to solve this problem, the consequence is even more serious to prediction in ungauged basins. If this argument is accepted a

hydrological modelers should seek methods to acquire a more realistic subgrid scale parameterization.

When analyzing physically based models we see that models such as SHE (Abbott *et al.*, 1986a; Abbott *et al.*, 1986b) TOPMODEL (Beven and Kirkby, 1979), IHDM (Rogers *et al.*, 1985) have no need, in theory, of precautionary calibration since the relative parameters offer a clear physical significance which makes an estimate of their values possible in relation to a knowledge of the basins characteristics. However, it seems to be necessary to differentiate between physically based in the sense of being based on defined assumptions and theories, and physically based in the sense of being consistent with observations. The fact that a model may be physically based in theories but not consistent with observations results primarily from the mismatch in scales between the scale of observable state variables and the scale of application.

Even in a fully distributed physically based hydrological model, the differential equations concerning the various hydrological processes (overland flow, infiltration, percolation etc.) are solved for the single cells in which the basin is subdivided, introducing a conceptualization of the phenomenon itself for hydrological processes (the heterogeneity of the hydrological quantities inside the cell are ignored). Conceptualizations introduced in this way, result in different performances in the models themselves with variations in the assumed scale. In catchment hydrology, the need is not much for a model that is theoretically acceptable, but for a model that is consistent with observations at the scale of interest (Beven, 2002). An alternative blueprint for a physically based hydrological model proposed by Beven (2002) is one that is acceptably consistent with the data.

TOPMODEL, in practice, represents an attempt

to combine the computational and parametric efficiency of a distribution function approach with the link to a physical theory and possibilities for more rigorous evaluation offered by a fully distributed model. Though it is used for a wide variety of application, it's dominating geomorphometric parameters that account for the hydrological similarity condition is also strongly influenced by the resolution of a DEM used. This results in parameter inconsistency and predictive uncertainty across scales.

In this study we focus on the influence of DEM resolution on dominating geomorphometric parameters - such as slope angle, upslope contributing area, which are considered as the main controls in a number of hydrological processes - and develop a method to downscale the topographic index of TOPMODEL by incorporating scaling laws. By using the method, the topographic index distribution of a fine resolution DEM is successfully derived by using only a coarse resolution DEM (Pradhan *et al.*, 2004). Then we develop a Scale Invariant TOPMODEL by coupling the method to downscale the topographic index distribution with TOPMODEL and it is shown that the Scale Invariant TOPMODEL is consistent with observation when applied at coarse resolution DEM with the parameter identified at fine resolution DEM.

2. Dependence of Topographic Index Distribution of TOPMODEL on DEM Resolution

The topographic index (Kirkby, 1975) of TOPMODEL is defined as

$$TI = \ln \left\{ \frac{a}{(\tan \beta)} \right\} \quad (1)$$

where a is the local up-slope catchment area per unit

contour length and β is the slope angle of the ground surface. TOPMODEL allows for spatial heterogeneity by making calculations on the basis of the topographic index distribution. The Topographic index is scale dependent which leads identified parameter values to be dependent on a DEM resolution. This makes difficult to use model parameter values identified with different resolution model. To overcome the problem, the scale invariant model of topographic index is proposed. To scale upslope contributing area per unit contour length a and slope angle of the ground surface β , a resolution factor and a scaled slope with a fractal method is introduced.

2.1 Theory of TOPMODEL

The topographic index defined by Equation (1) describes the tendency of water to accumulate and to be moved down slope by gravitational forces. For steep slopes at the edge of a catchment, a is small and β is large which yields a small value for the topographic index. High index values are found in areas with a large up-slope area and a small slope, e.g. valley bottoms. The TOPMODEL theory can be formulated by the concept of local saturation deficits, water needed for saturation up to surface.

Following Beven and Kirkby (1979), Beven (1986) and Beven (2000), subsurface flow rate $q_b(i, t)$, per unit contour length [L^2T^{-1}] can be related to local soil storage deficit below surface saturation or depth to water table $S(i, t)$ [L] by

$$q_b(i, t) = T_o \tan \beta_i e^{-S(i, t)/m} \quad (2)$$

where, i is any point in a catchment, $\tan \beta_i$ is slope angle, T_o is the lateral (horizontal) transmissivity when the soil is just saturated to the surface-zero storage deficit- [L^2T^{-1}] and $T_o \approx K_o/f$, K_o is saturated conductivity at the soil surface and f is a parameter. m is a decay factor of saturated

transmissivity of soil with respect to saturation deficit, also with dimensions of length [L]. Under quasi-steady state conditions, due to an assumed spatially uniform recharge rate, R [LT^{-1}]

$$a_i R = T_o \tan \beta_i e^{-S(i,t)/m} \quad (3)$$

where, a_i is the area draining through i per unit contour length [L^2]. Equation (3) can be rearranged to Equation (4).

$$S(i,t) = -m \left[\ln \left\{ \frac{a_i}{(T_o \tan \beta_i)} \right\} + \ln R \right] \quad (4)$$

Integrating the point deficits over the catchment area of interest A , the spatial mean deficit $\bar{S}(t)$ is given by

$$\bar{S}(t) = \frac{1}{A} \int_A S(i,t) dA = \frac{1}{A} \int_A -m \ln \left(\frac{a_i R}{T_o \tan \beta_i} \right) dA \quad (5)$$

and substituting for $\ln R$ from Equation (4)

$$\bar{S}(t) = S(i,t) - m\gamma + m \ln \left\{ \frac{a_i}{(T_o \tan \beta_i)} \right\} \quad (6)$$

where, $\gamma = \frac{1}{A} \int_A \ln \left\{ \frac{a_i}{(T_o \tan \beta_i)} \right\} dA$ is a constant for the basin. Equation (4) and (5) yield a relation between $\bar{S}(t)$ and $S(i,t)$ at each single location i .

The combined soil topographic index part in Equation (6) is defined as

$$\ln(a_i / T_o \tan \beta_i) \quad (7)$$

Underlying the development of Equation (6) is an assumption that all points with the same combined soil topographic index value shown by Equation (7) are hydrologically similar (Beven, 1986). Subsurface contributions to streamflow, $Q_b(t)$ [LT^{-1}] (Beven, 1986; Beven, 2000) can be derived from Equation (6) as

$$Q_b(t) = e^{-\gamma} e^{-\bar{S}(t)/m} \quad (8)$$

Considering lateral transitivity to be constant in a catchment or subcatchment, then the key role for hydrological similar condition is played by the distribution function of the topographic index. The bitter fact is that higher frequency topographic information contained in topographic index is lost as the larger sampling dimensions of the grids act as filter. This makes the hydrological similarity condition accounting combined soil-topographic index in Equation (7) to vary with the variation in a DEM resolution used. To overcome this problem, this research has developed a method to downscale a topographic index distribution.

2.2 DEM resolution effect on topographic index

Fig.1 shows the density function of the topographic index at four different DEM resolutions in the Kamishiiba catchment (210 km²) in Japan without taking into account the scale effect. Distinct shift of the topographic index density functions towards the higher value is seen as the resolution of DEM becomes coarser. This is a clear indication of the lost of higher frequency topographic information as the larger sampling dimensions of the grids act as

Table 1 DEM resolution effect on topographic constant, λ , value in Kamishiiba catchment

DEM Resolution [m]	50	150	450	600	1000
Topographic constant λ [$\ln(\text{m}^2)$]	6.076	7.423	9.222	9.622	10.353

filter. Table 1 shows the distinct effect of DEM resolution on a spatial mean value of the topographic index λ in Equation (9).

$$\lambda = \frac{1}{A} \int_A \ln(a_i / \tan \beta_i) dA \quad (9)$$

Only available DEM data for most of the parts of the world that covers ungauged basins of developing and underdeveloped countries is that of 1km x 1km grid resolution. Analyzing Fig. 1 and Table 1, we can readily imagine the blunder in predicting ungauged basins using only coarse resolution DEM with the parameter values identified at the finer resolution DEMs.

3. Development of the Method to Downscale Topographic Index

A method to downscale topographic index of TOPMODEL has been developed by combining the following two parts of solutions.

3.1 Resolution factor in topographic index

It is observed that the small contributing area is entirely lost when the resolution of DEM gets coarser. Fig. 1 clarifies that higher frequency topographic information contained in a topographic index distribution is lost. In Fig. 1, the peak value of the density distribution of the topographic index for 50m grid resolution DEM is 4.2 [$\ln(\text{m}^2)$] and the peak value for 1000m grid resolution DEM is 8.6 [$\ln(\text{m}^2)$].

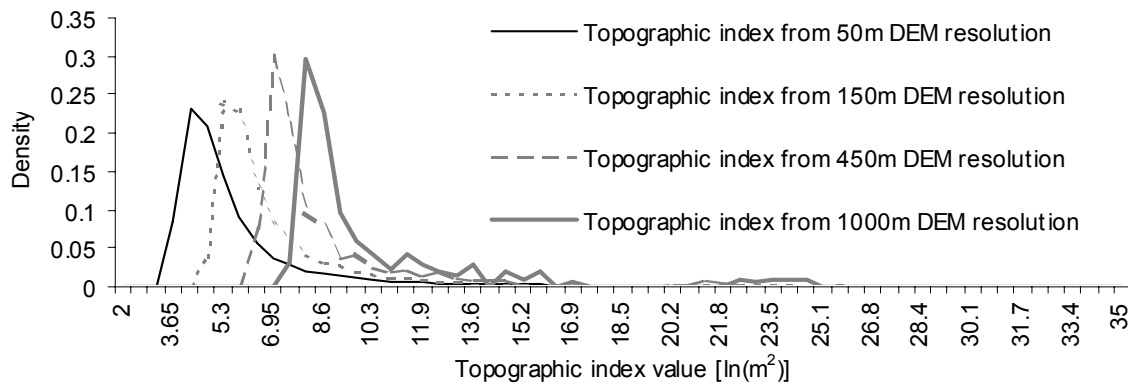


Fig. 1 Effect of DEM resolution on density distribution of topographic index

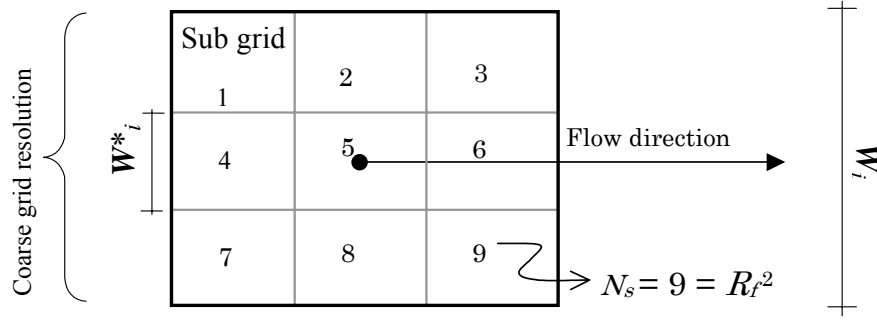


Fig. 2 Sub grids within coarse grid resolution for introducing resolution factor in topographic index

In fact the smallest contributing area derived from a DEM resolution is a single grid area of the DEM at that resolution. Thus the area smaller than this grid resolution is completely lost. However, as we use finer resolution DEM, the smaller contributing area that is the area of finer grid resolution is achieved. From this point of view we introduced a number of sub grids N_s (see Fig. 2) concept in topographic index as shown in Equation (10).

$$TI = \ln \left\{ \frac{C_i}{(W^*_i N_s \tan \beta_i)} \right\} \quad (10)$$

where TI is the topographic index. C_i is the upslope contributing area of the coarse resolution DEM and W^*_i is the unit contour length of target resolution DEM. N_s is the total number of subgrids within a coarse resolution grid and i is a location in a catchment.

Fig. 2 shows 9 subgrids within a coarse resolution grid. The area of the coarse resolution grid shown in Fig. 2 itself is the smallest contributing area for that DEM resolution. When this area of coarse resolution DEM is divided by the number of sub grids N_s , i.e. 9 in Fig. 2, area of a sub grid as smallest contributing area for the target DEM resolution is obtained. Moreover, in Equation (10), the unit contour length of coarse resolution DEM, W_i , is replaced by the unit contour length of targeted DEM resolution W^*_i (see

Fig. 2) to derive the lost portion of the finer values of contributing area per unit contour length.

The density distribution of the higher values of contributing area per unit contour length is found lower in case of finer grid resolution DEM than that of coarser grid resolution DEM. This is the reason for the topographic index derived from coarser resolution DEM to shift towards the higher value throughout the density distribution, not only at the peak of the density distribution, than the topographic index derived from finer resolution DEM (see Fig. 1). Structure of Equation (10) having logarithmic function, proportionately pulled back this higher topographic index density towards that of finer resolution DEM.

If we consider resolution factor R_f as

$$R_f = \frac{\text{Coarse DEM Resolution}}{\text{Target DEM Resolution}} = \frac{W_i}{W^*_i} \quad (11)$$

then it is clear from Figure 2 that

$$N_s = R_f^2 \quad (12)$$

Equation (11) and (12) yield

$$W_i R_f = W^*_i N_s \quad (13)$$

From, Equation (10) and Equation (13) resolution factor is introduced in topographic index as

$$TI = \ln \left\{ \frac{C_i}{(W_i R_f \tan \beta_i)} \right\} \quad (14)$$

3.2 Fractal method for scaled steepest slope

The underestimation of slopes when using the coarse resolution DEMs can seriously affect the accuracy of hydrologic and geomorphological models (Zhang *et al.*, 1999). To scale the local slope, we followed the fractal theory in topography and slope proposed by Klinkenberg and Goodchild (1992) and Zhang *et al.*, (1999) and developed a modified fractal method for steepest descent slope.

(1) Fractal method for average slope estimation proposed by Zhang et al. (1999)

The variogram technique can be used to calculate the fractal dimension in a region when the log of the distance between samples is regressed against the log of the mean squared difference in the elevations for that distance.

The variogram equation used by Klinkenberg and Goodchild (1992) to calculate the fractal dimension of topography is:

$$(Z_p - Z_q)^2 = kd_{pq}^{(4-2D)} \quad (15)$$

where Z_p and Z_q are the elevations at points p and q , d_{pq} is the distance between p and q , k is a constant and D is fractal dimension. Topographic fractal properties of Equation (15) can be used to scale slope as follows:

$$\frac{(Z_p - Z_q)}{d_{pq}} = \alpha d_{pq}^{(1-D)} \quad (16)$$

where $\alpha = \pm k^{0.5}$ is a constant. Because the left part of the above equation represents the surface slope, it can be assumed that the slope value θ is associated with its corresponding scale, grid size, d by the equation:

$$\theta = \alpha d^{(1-D)} \quad (17)$$

This implies that if topography is unifractal in a specified range of measurement scale, slope will then be a function of the measurement scale (Zhang *et al.*, 1999). However, it is impossible to predict the spatial patterns of slopes due to the single value of the fractal dimension and the coefficient in the fractal slope equation for the whole DEM. To overcome this problem Zhang *et al.* (1999) proposed that the coefficient α and fractal dimension D of Equation (17) are mainly controlled by standard deviation of the elevation of the sub regions in a DEM and brought out the regressed relations between α and D separately with the standard deviation of the elevation. In deriving the regressed relation, Zhang *et al.*, (1999) considered the smallest sub area (window) to be composed of 3 x 3 pixels. Hence elevations of nine neighboring grids in the DEM are taken to obtain the standard deviation of the elevation for a sub area.

It is found that the slope derived from the method by Zhang *et al.*, (1999) tend to match only with the average slope within the 3 x 3 moving window pixels of the coarse resolution DEM but completely failed to take into consideration of the steepest descent slope defined as the direction of the maximum drop from center pixel to its eight nearest neighbors. Steepest descent slope also known as D8 method (O'Callaghan and Mark, 1984; Jenson and Domingue, 1988; Martz and Garbrecht, 1992) has a significant

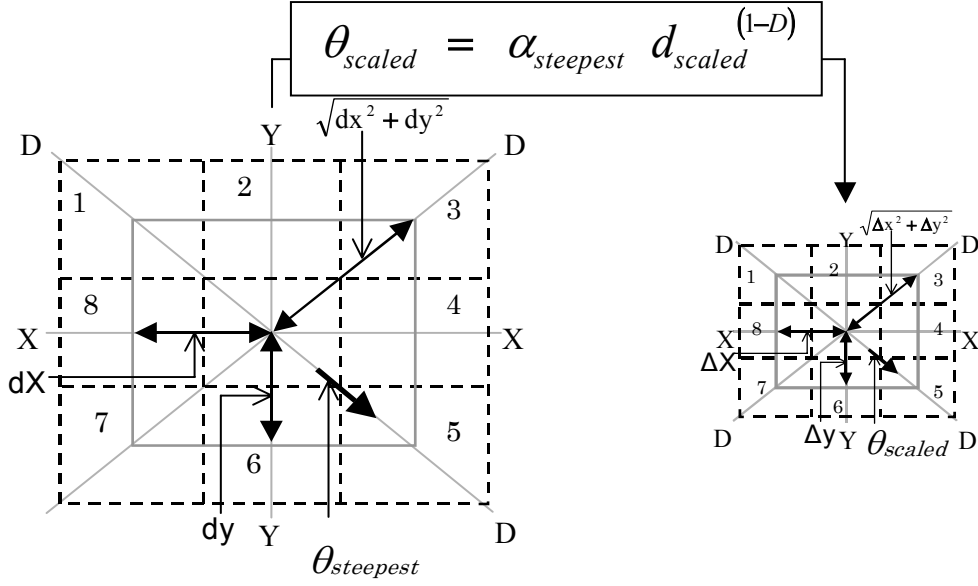


Fig. 3 Fractal method for scaled steepest slope at a location I of the 3 x 3 moving window pixels

role in hydrological modeling that incorporates DEM. Thus we propose a modified fractal method for steepest descent slope.

(2) Fractal method for steepest descent slope

In this research, a modified model for fractal method to account for the steepest slope change due to change in DEM resolution has been developed which is described in the following points:

(a) Unlike the distance d of Equation (17) be represented by constant grid size, in every step (location) in a 3 x 3 moving window pixels, this distance d of Equation (17) is provided as the steepest slope distance ($d_{steepest}$). Fig. 3A shows the steepest slope distance $d_{steepest}$ to be dx , dy and $\sqrt{dx^2 + dy^2}$ according to the direction of steepest descent of the slope in X-axis, Y-axis and diagonal axis DD respectively.

(b) It is found that there is not much variation in standard deviation of elevation from high resolution DEM to low resolution DEM in the same sub-area. Fractal dimension D is related to standard

deviation of elevation σ [m] in 3 x 3 moving window pixels as per Zhang *et al.*, (1999).

$$D = 1.13589 + 0.08452 \ln \sigma \quad (18)$$

(c) The fluctuations of the coefficient α values were found very high from one local place to another in comparison to D value in Equation (17). Unlike the method by Zhang *et al.*, (1999) in which α values are derived from standard deviation σ of the elevation in 3 x 3 moving window pixels), we developed a new method in which coefficient α values are derived directly from the steepest slope of the available coarse resolution DEM, keeping the fact that steepest slope itself represents the extreme fluctuation. The modified equation is:

$$\theta_{steepest} = \alpha_{steepest} d_{steepest}^{(1-D)} \quad (19)$$

As for example in Fig. 3A, where the steepest slope is shown in diagonal direction, $\alpha_{steepest}$ at that location i

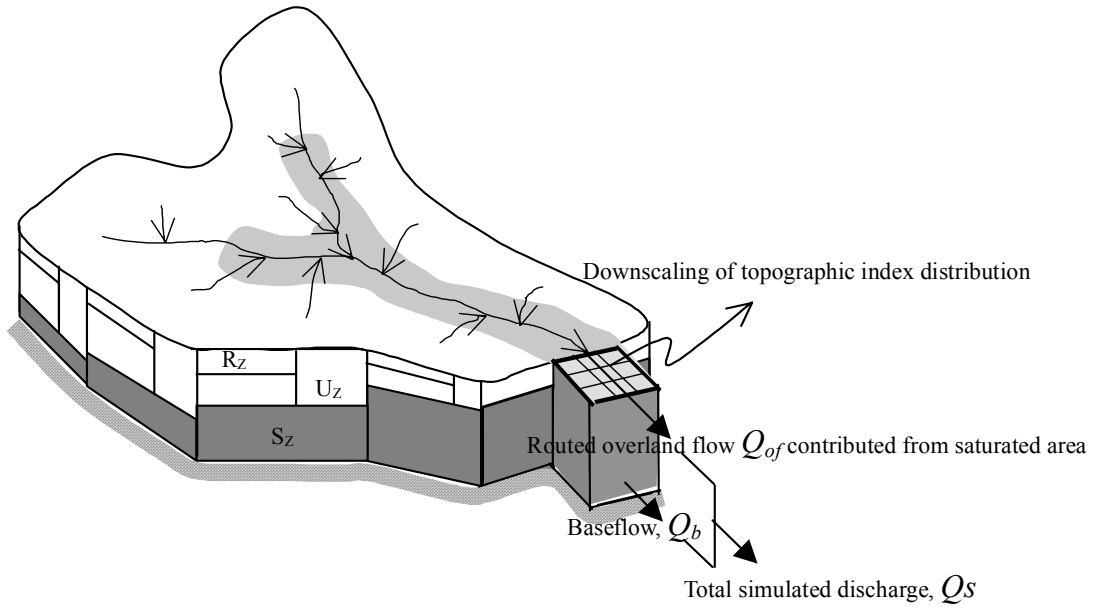


Fig. 4 Development of the Scale Invariant TOPMODEL

is given by, $\alpha_{steepest} = \frac{\theta_{steepest}}{(\sqrt{dx^2 + dy^2})^{(1-D)}}$ where dx

and dy are the steepest slope distances of the coarse resolution DEM in X-axis and Y-axis.

(d) While downscaling, the distance variation in the target resolution DEM is made as per the direction of the steepest slope in the coarse resolution DEM. Hence in Fig. 3B the down scaled steepest slope θ_{scaled} is shown in the same direction to that of the coarse resolution DEM steepest slope (Fig. 3A). Considering Fig. 3B, the downscaled steepest slope θ_{scaled} is given as

$$\theta_{scaled} = \alpha_{steepest} d_{scaled}^{(1-D)} \quad (20)$$

where $d_{scaled} = \sqrt{\Delta x^2 + \Delta y^2}$ in Fig. 3B and Δx , Δy are the steepest slope distances of the target resolution DEM in X-axis and Y-axis respectively.

(3) Scaled topographic index distribution

By combining Equation (14) and Equation (20), the method to downscale the topographic index which includes resolution factor to account for the effect of scale in up slope contributing area per unit contour length and a fractal method for scaled steepest slope as an approach to account for the effect of scale on slope is given by Equation (21).

$$(TI)_{scaled} = \ln \left[\frac{C_i}{\{W_i R_f (\tan \beta_i)_F\}} \right] \quad (21)$$

where, $(TI)_{scaled}$ is the scaled topographic index and $(\tan \beta_i)_F$ is θ_{scaled} of Equation (20) which is the scaled steepest slope by fractal method.

4. Scale Invariant TOPMODEL

Total runoff is calculated as the sum of two flow components: saturation excess overland flow from

Table 2 Topographic constant, λ , value for scaled DEM from 1000 m grid resolution to finer grid resolutions in Kamishiiba catchment

Topographic constant, λ [$\ln(\text{m}^2)$], value for scaled DEM from 1000 m grid resolution to											
50 m target grid resolution	150 m target grid resolution				450 m target grid resolution	600 m target grid resolution					
6.474	7.573				9.11	9.604					

variable contributing areas (Dunne and Black, 1970) and subsurface flow from the saturated zone of the soil as shown in Fig. 4. Area with $S(i,t) \leq 0$ (in Equation 6) are contributing areas for saturation excess overland flow. Following Equation (6), the dependency of $S(i,t)$ on other variables in TOPMODEL is shown as

$$S(i,t) = f(\bar{S}(t), To, TI, \lambda, m) \quad (22)$$

Again from Equation (8) the dependency of subsurface flow from the saturated zone (S_z [m] in Fig. 4) in TOPMODEL, $Q_b(t)$ is written as

$$Q_b(t) = g(To, \lambda, m, \bar{S}(t)) \quad (23)$$

In Equation (22) and Equation (23) the only independent heterogeneity accounting observable variable is the topographic index TI . To , λ , m and $\bar{S}(t)$ in the catchment or subcatchment are directly influenced by the topographic index value, which changes with the resolution of a DEM used. This makes recalibration in the model compulsory as the scale of observable state variables and scale of application are mismatched. Thus in the TOPMODEL concept, to make topographic index value scale invariant, Equation (1) has been replaced by Equation (21) that leads to the development of

Scale Invariant TOPMODEL. The scale invariant function defined by Equation (21) is based on scale laws and does not add any extra parameter burden when coupled with TOPMODEL.

Root zone store, R_z [m] in Fig. 4 for each topographic index value is depleted only by evapotranspiration, and that water is added to the unsaturated zone drainage storage, U_z [m] in Fig. 4, only once the root zone reaches field capacity or maximum root zone storage, R_{zmax} [m]. The drainage from the unsaturated zone is assumed to be essentially vertical and drainage flux per unit area q_v [LT^{-1}] is calculated for each topographic index class which is controlled by $S(i,t)$ and saturated conductivity at the soil surface Ko (Beven, 1986) as

$$q_v(i,t) = \min \left\{ Ko e^{-S(i,t)/m}, UZ(i,t) \right\} \quad (24)$$

where $Ko \approx To f$ and f is a parameter. Initial condition for average saturation deficit $\bar{S}(0)$ is derived from Equation (8) taking $Q_b(0)$ as initial observed discharge (Beven, 1987). \bar{S} in the successive time step is calculated by Equation (25).

$$\bar{S}(t+1) = \bar{S}(t) - Q_v(t) + Q_b(t) \quad (25)$$

where $Q_v(t)$, total input to groundwater from the

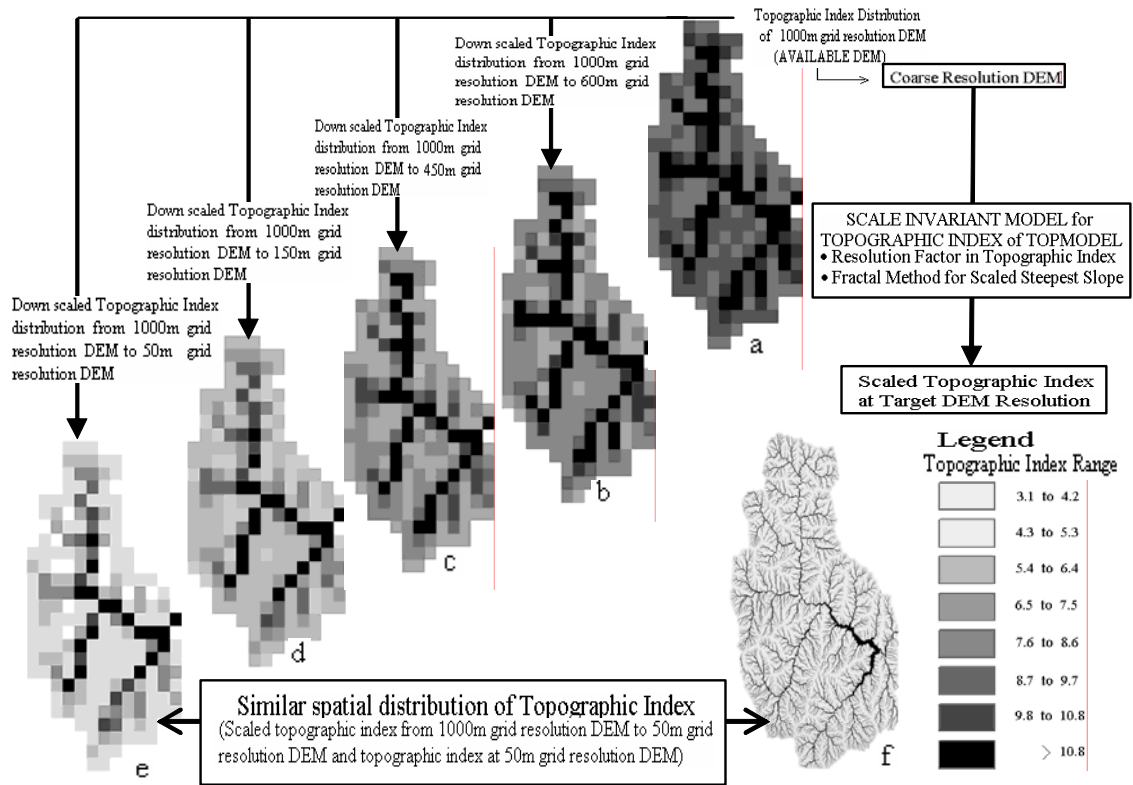


Fig. 5 Spatial distribution of scaled topographic index applied to Kamishiiba catchment (210 km²). (a) topographic index distribution using 1000m DEM resolution, (b) scaled topographic index distribution obtained from 1000m DEM resolution to 600m DEM resolution, (c) scaled topographic index distribution from 1000m DEM resolution to 450m DEM resolution, (d) scaled topographic index distribution from 1000m DEM resolution to 150m DEM resolution, (e) scaled topographic index distribution from 1000m DEM resolution to 50m DEM resolution, (f) topographic index distribution using 50m DEM resolution

unsaturated zone, is the sum of $q_v(t)$ over all grids in the catchment and $Q_b(t)$ is the groundwater discharge to the stream. Muskingum-Cunge routing method is used for hill slope channel routing (Cunge, 1969).

5. Results and Discussion

The method to downscale the topographic index and the Scale Invariant TOPMODEL are applied to Kamishiiba catchment (210 km²), Japan. Details of the results and discussion are presented in the following paragraphs.

5.1 Application of the method to downscale the topographic index distribution

The method to downscale the topographic index of TOPMODEL is applied to Kamishiiba catchment (210 km²). Table 2 shows the scaled topographic constant λ from 1000m grid resolution DEM to various target DEM resolutions by applying the scale invariant model. The downscaled values of λ from 1000m grid resolution to finer DEM resolutions in Table 2 are almost equal to the values of λ in Table I derived from that fine grid resolution DEMs.

Fig. 5a is the topographic index distribution

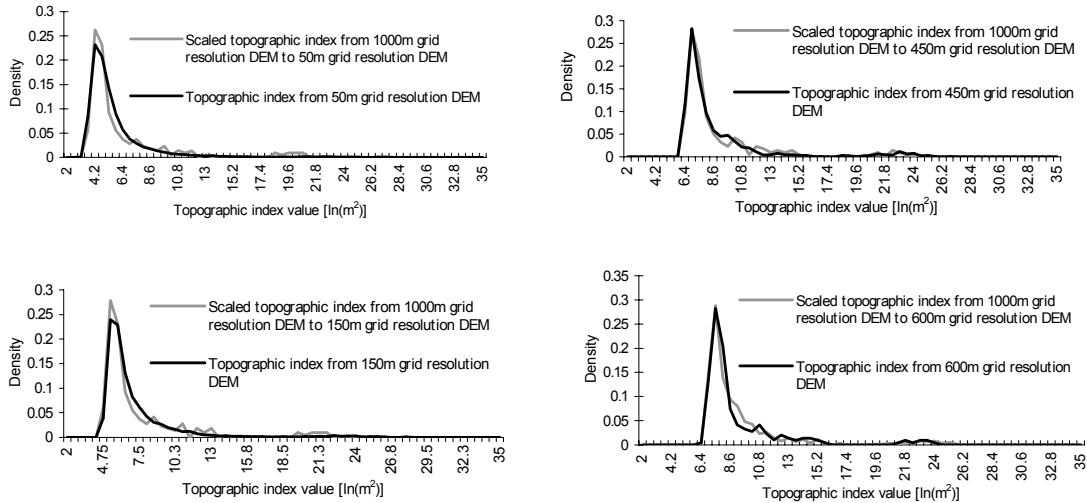


Fig. 6 Comparison of density function of scaled topographic index from 1000m grid resolution DEM to finer grid resolution DEM and the density function of the topographic index at that fine scale in Kamishiiba catchment (210 km²)

using 1000m DEM. Fig. 5 b, c, d and e are the scaled topographic index distribution obtained by using the scale invariant model with the same 1000m grid resolution DEM to 600m, 450m, 150m and 50m grid resolution DEM respectively. Fig. 5f is the topographic index distribution using 50m DEM. Distinct difference can be seen between spatial distribution of the topographic index in Fig. 5a and Fig. 5f that are from 1000m-grid resolution DEM and 50m-grid resolution DEM respectively. The spatial distribution of topographic index displayed by Fig. 5e has matched the existing reality displayed by Fig. 5f.

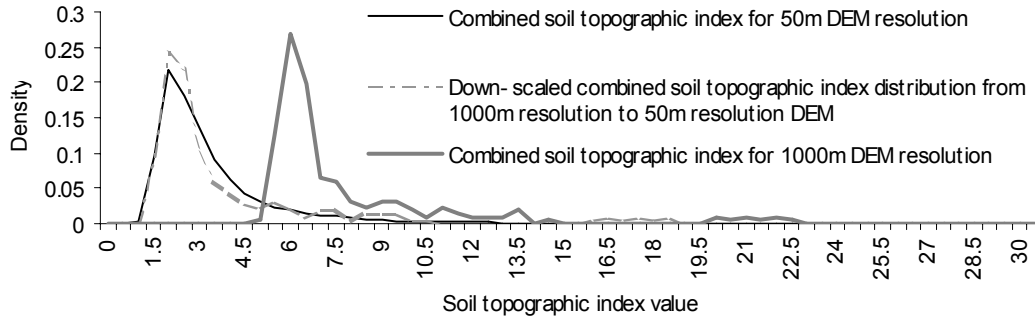
Fig. 6 shows the perfect fit of density function of scaled topographic index distribution from 1000m grid resolution DEM to various grid resolution DEMs by using scale invariant model. It is found that in the finer resolution range of DEM, between 50m-grid resolution DEM and 150m-grid resolution DEM where the slope obtained is more precise and does not vary significantly, resolution factor (R_r) alone played the dominant role in the scale invariant model. Above 150m DEM scale, effect of resolution on slope is found distinct.

5.2 Hydrological similarity concept of TOPMODEL across different DEM resolutions in the catchment

Specifying a spatial distribution for T_o being much more problematic, in most applications, it has been assumed to be spatially homogeneous, in which case the similarity index defines by Equation (7) reduces to the form $a / (\tan \beta)$.

But when the resolution of the DEM change, the spatial distribution of topographic index also change. In this scenario, the same effective parameter value of T_o for changed DEM resolutions and similarity index reduced to the form $a / (\tan \beta)$ cannot fulfill the hydrological similarity concept of TOPMODEL across different DEM resolutions in the catchment.

In the combined soil topographic index for 50m DEM resolution in Fig. 7, the effective parameter value of lateral transmissivity of soil is 9.8 m²/s which is calibrated at 50m DEM resolution of Kamishiiba catchment (210 km²). Keeping the same effective parameter value of T_o obtained from 50m grid resolution DEM (9.8 m²/s) and applied in combined soil topographic index distribution where the topographic index distribution is from 1000m grid



resolution DEM (see Fig. 7) has distinctly shifted the combined soil topographic index distribution towards the much higher values from that of combined soil topographic index distribution from 50m DEM resolution. Thus keeping the same effective parameter value of T_o for changed DEM resolutions and similarity index reduced to the form $a/(\tan \beta)$ cannot fulfill the hydrological similarity concept of TOPMODEL across different DEM resolutions.

It is also observed that increasing in effective parameter value of lateral transmissivity of soil pulled back the higher valued distribution of combined soil topographic index from 1000m grid resolution DEM towards combined soil topographic index from 50m grid resolution DEM, but the parameter value tends to exceed more than $100\text{m}^2/\text{hr}$ —exceeding the physically acceptable range—before the combined soil topographic index distribution from 50m grid resolution and 1000m grid resolution DEM matched. In this case the value of T_o parameter determined by model calibration is rather to compensate for the overestimation of the combined soil-topographic index $\ln[a / T_o (\tan \beta)]$ in Equation (7) obtained from higher resolution DEM.

For the solution of the discussed problems, the method to downscale topographic index distribution is applied to downscale the topographic index distribution from 1000m-grid resolution DEM to 50m-grid resolution DEM. This downscaled topographic index distribution from 1000m-grid

resolution DEM to 50m-grid resolution DEM is then coupled with the effective parameter value of lateral transmissivity of soil ($T_o=9.8 \text{ m}^2/\text{hr}$) calibrated at 50m-grid resolution DEM to obtain scaled soil topographic index for 50m-grid resolution DEM (see Fig. 7). In Fig. 7 it is shown that scaled soil topographic index distribution has matched the soil topographic index at 50m-DEM resolution. At this point, the method to downscale topographic index distribution has solved two problems. Firstly, it fulfilled the hydrological similarity concept of TOPMODEL across different DEM resolutions of a catchment by keeping the same effective parameter value of T_o for changed DEM resolutions and similarity index reduced to the form $a/(\tan \beta)$. Secondly, it has given consistency to the effective parameter with observations at the scale of interest.

5.3 Application of Scale Invariant TOPMODEL

In Fig. 8, A(I), A(II) and A(III) are the simulation result from 50m DEM resolution TOPMODEL; B(I), B(II) and B(III) are the simulation results from 1000m DEM resolution TOPMODEL; C(I), C(II) and C(III) are the simulation results from Scale Invariant TOPMODEL, applied at 1000m DEM resolution and the topographic index downscaled to 50m DEM resolution, that belong to rainfall events Event(1), Event(2) and Event(3) respectively.

For the simulation results shown in Fig. 8 A(I),

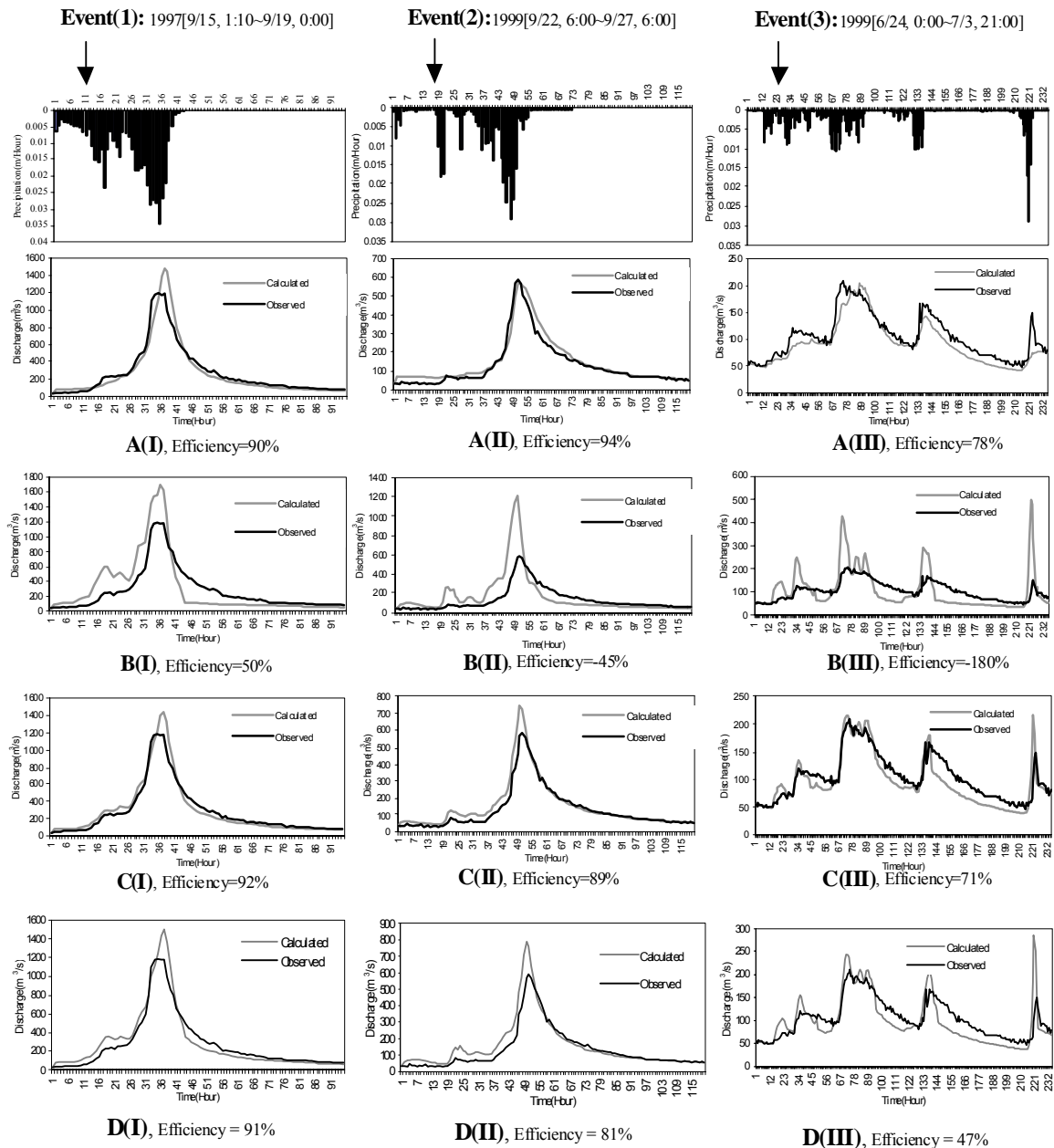


Fig. 8 Simulation results of TOPMODEL (with and without coupling the downscaling method of topographic index) applied to Kamishiiba catchment (210 km^2). A(I), A(II), A(III) are the simulation results from 50m DEM TOPMODEL. B(I), B(II), B(III) are the simulation results from 1000m DEM TOPMODEL without scale invariant model for topographic index. C(I), C(II), C(III) are the simulation results from Scale Invariant TOPMODEL at 1000m DEM resolution and topographic index downscaled to 50m DEM resolution. Same set of effective parameter values, identified by 50m DEM resolution TOPMODEL, is used for all the simulation results in A(I), A(II), A(III), B(I), B(II), B(III), C(I), C(II) and C(III). D(I), D(II) and D(III) are the simulation results from 1000m DEM TOPMODEL without scale invariant model for topographic index and with parameters recalibrated at 1000m DEM resolution

A(II), A(III), B(I), B(II), B(III), C(I), C(II) and C(III), the used effective parameter of TOPMODEL, see Table 3, are identified by 50m DEM resolution TOPMODEL. But, D(I), D(II) and D(III) are the simulation results from 1000m DEM resolution TOPMODEL where parameters used are identified at 1000m DEM resolution.

Although the Identified effective parameters in Table 3 are calibrated by 50m DEM resolution

TOPMODEL in Event (2), Fig. 8A(II), which gave the Nash efficiency of 94%, the importance is also given to the model consistency of 50m DEM resolution TOPMODEL with the same set of parameters to other events (in Event (1), Fig. 8A(I), Nash efficiency is 90% and in Event (3), Fig. 8A(III), Nash efficiency is 78%). Parameter value for m was derived also from the first-order hyperbolic function that fitted the recession curve obtained from the observed discharge of rainfall event (1). The derived value of the parameter m by the recession analysis (Ambrose *et al.*, 1996; Güntner *et al.*, 1999), i.e. 0.078 m, is found near to the calibrated parameter value of m by 50m DEM resolution TOPMODEL, i.e. 0.07 m. The value for parameter f that relates To and Ko is kept as unity in all the simulations.

Comparing Fig. 8B(I), B(II), B(III) with Fig. 8A(I), A(II), A(III) respectively it is seen that the magnitudes of the differences in TOPMODEL predictions based on different DEM resolutions, with the same set of parameter values, are large. In Fig.

8B(I), B(II) and B(III), the simulated hydrograph shows overestimation or underestimation of the discharge in comparison with the observed flows and also in comparison with the simulated hydrographs in Fig. 8A(I), A(II) and A(III) respectively.

The simulated discharge in Fig. 8B(I), B(II) and B(III) are very sensitive to rainfall showing overestimation of discharge in the rainfall duration and underestimating of discharge as soon as the rainfall stopped or diminished. Because of this inconsistency of 1000m DEM resolution TOPMODEL prediction, keeping same parameter values identified at 50m DEM resolution TOPMODEL, the Nash efficiency in Fig. 8B(I), B(II), B(III) drastically dropped down to 50%, -45% and -180% respectively.

5.4 Discussions

It is a bitter fact of the scale effect where hydrological models like TOPMODEL being physically based on defined assumptions and theory completely fails to justify itself as physically based practically, in the sense of being consistent with observations.

Earlier in Table 1 we showed that as the resolution of DEM gets coarser, a spatial mean value of topographic index, λ in Equation (9), increases. As λ value increased, the predicted mean depth to the water table decreased, or average saturation deficit shifted from higher value towards zero value. In the

Table 3 Effective parameter values identified by 50m DEM resolution TOPMODEL and used (same parameter values) for different events and different DEM resolutions in Kamishiiba catchment

Lateral transmissivity of soil at saturation condition, To [m^2/hr]	decay factor of lateral transmissivity with respect to saturation deficit, m [m]	Maximum root zone storage, Rz_{max} [m]
9.8	0.07	0.001

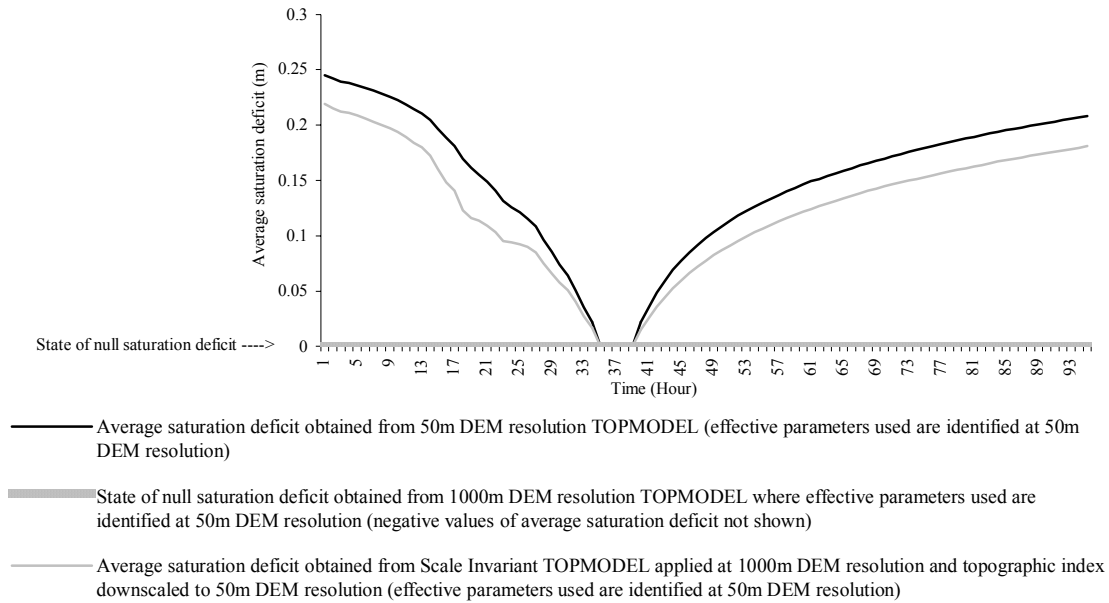


Fig. 9 Comparison of average saturation deficit in Kamishiiba catchment (210 km²) obtained from 50m DEM resolution TOPMODEL, 1000m DEM resolution TOPMODEL and Scale Invariant TOPMODEL applied at 1000m DEM resolution with scaled topographic index to 50m DEM resolution. In all these cases the applied effective parameters are identified by 50m DEM resolution TOPMODEL

model zero saturation deficit is the state of the vertical soil profile to be completely saturated up to surface. Any further rainfall after zero local saturation deficit state is directly contributed as surface runoff, local saturation deficit is directly related to average saturation deficit by Equation (6). Lower the saturation deficit, the maximum daily flow and the variance of the daily flow increased. This is because more the initial saturation deficit value shifts towards the zero saturation deficit condition the lesser is the amount of rainfall input needed to produce the surface runoff which accounts for the peak flows (see Fig. 9).

Fig. 9, shows that the average saturation deficit predicted by 1000m DEM resolution TOPMODEL, by keeping the effective parameter identified at 50m DEM resolution, has unrealistically reached the state of complete saturation throughout the simulation period. This indicates that a large part of the catchment is unrealistically at the state of complete

saturation. This is why the saturated area contributing the surface runoff is unrealistically large within the catchment that is overestimating the simulated discharge during rainfall duration in Fig. 8B(I), B(II) and B(III). On the other hand, in TOPMODEL, topographic constant λ affects the maximum subsurface flow rate (see Equation (8)); the higher the λ value, the lower the maximum subsurface flow rate. Table 1 shows that value of λ increased from 6.076 [$\ln(\text{m}^2)$] to 10.353 [$\ln(\text{m}^2)$] as the resolution of DEM changed from 50m to 1000m. Thus at 1000m DEM resolution, the subsurface flow rate produced by the TOPMODEL is much lower which is only the simulated discharge at no rainfall hours. This is the reason for the underestimation of the simulated discharge during no rainfall hours in Fig. 8B(I), B(II) and B(III).

The saturated condition found through out the simulation period shown in Fig. 9 when analyzing the saturation deficit of 1000m DEM resolution

TOPMODEL is because of the reason that higher the topographic constant λ value lower the capacity to conduct water down slope through subsurface flow paths (Equation (8)) and therefore having a lower saturation deficit. Zhang and Montgomery (1994), Wolock and Price (1994) have also showed that increasing the coarseness of DEM data resolution tended to decrease the mean depth to water table and increase the peak flow but did not come up with any effective solution approach.

The Scale Invariant TOPMODEL is applied at 1000m DEM resolution of Kamishiiba catchment. The Scale Invariant TOPMODEL downscaled the topographic index from 1000m-grid resolution DEM to 50m-grid resolution DEM. Table 2 shows that the downscaled λ from 1000m DEM resolution to 50m DEM resolution is very close to λ value at 50m DEM resolution; Fig. 5 and Fig. 6 shows the similar spatial distribution of scaled topographic index from 1000m-grid resolution DEM to 50m-grid resolution DEM and topographic index at 50m-grid resolution DEM. Thus in Fig. 9, the average saturation deficit simulated from Scale invariant TOPMODEL is quite similar to average saturation deficit simulated by 50m DEM resolution TOPMODEL. Because of the successful achievement of the topographic index distribution and the average saturation deficit produced by 50m-grid resolution DEM by using only 1000m-grid resolution DEM shown in Fig. 5, Fig. 6 and Fig. 9, the Scale Invariant TOPMODEL applied at 1000m DEM resolution simulated discharge in Fig. 8C(I), C(II) and C(III) that matched with the simulated discharge of 50m DEM resolution TOPMODEL in Fig. 8A(I), A(II) and A(III) respectively. Thus the Nash efficiency in Fig. 7C(I), C(II) and C(III) are 92%, 89% and 71% respectively.

Fig. 8 D(I), D(II) and D(III) are the simulation results of 1000m DEM resolution TOPMODEL that is recalibrated at 1000m DEM resolution. The used

recalibrated parameter is from the Event (1) in Fig. 8 D(I) that gave the highest Nash efficiency, 91%, among all the three events. The recalibrated value of T_o at 1000m DEM resolution shoot up from 9.8 m²/hr (the calibrated value by 50m DEM resolution TOPMODEL) to 97 m²/hr. What is clear from this analysis is that an increase in the mean of $\ln\{a/(\tan \beta)\}$, λ , caused by using a coarser scale DEM would have been compensated for by an increase in calibrated value of T_o but then the parameter value would exceed physically acceptable range making the problem of false assumptions less restrictive than it might otherwise be, since calibration can often compensate for such deficiencies.

Also in Fig. 8 D(II) and D(III) the recalibrated parameter at 1000m DEM resolution is used. The Nash efficiency obtained from Fig. 8 D(II) and D(III) are 81% and 47% respectively. Though recalibrated parameter is used in Fig. 8 D(I), D(II) and D(III), the Nash efficiency is found always lower than in Fig. 8 C(I), C(II) and C(III). This makes clear that for different rainfall events in the same catchment, the performance of the 1000m DEM resolution TOPMODEL with the parameter calibrated at 1000m DEM resolution is less consistent than that of the performance of the Scale Invariant TOPMODEL applied at 1000m DEM resolution and with the parameter identified at 50m DEM resolution.

The burden of parameter uncertainty and model inconsistency brought by the compulsion to recalibrate or by the application of the model parameter identified at coarse resolution DEM is solved by the Scale Invariant TOPMODEL. It is shown that the Scale Invariant TOPMODEL is consistent with observations (observed discharge data) although scale of observable state variables and scale of application are mismatched.

6. Conclusion

This research has developed a Scale Invariant TOPMODEL to fulfill the need of a physically based hydrological model, which is independent of DEM resolution effects and consistent with observations although scale of observable state variables and scale of application are mismatched. Analyzing the scale laws this research has developed concept of resolution factor to account for the effect of scale in up slope contributing area per unit contour length in topographic index and a fractal method for scaled steepest slope as an approach to account for the effect of scale on slopes, which are combined to develop the method to downscale topographic index distribution. The method to downscale the topographic index plays the role of scale invariant function in this newly developed Scale Invariant TOPMODEL. It is hoped that the findings of this research seeks its applicability as a tool to a wider range of boundary as per the scale problems in hydrological processes and solution approach is concerned.

References

- Abbott, M., B., Bathurst, J., C., Cunge, J., A., O'Connell, P., E. and Rasmussen, J. (1986a): An introduction to the European Hydrological System – Système Hydrologique Européen, SHE, 1: History and Philosophy of a Physically-Based, Distributed Modelling System, *Journal of Hydrology*, Vol. **87**, pp. 45-59.
- Abbott, M., B., Bathurst, J., C., Cunge, J., A., O'Connell, P., E. and Rasmussen, J. (1986b): An introduction to the European Hydrological System – Système Hydrologique Européen, SHE, 1: History and Philosophy of a Physically-Based, Distributed Modelling System, *Journal of Hydrology*, Vol. **87**, pp. 61-77.
- Ambroise, B., Beven, K. and Freer, J. (1996): Towards a generalization of the TOPMODEL concepts: topographic indices of hydrologic similarity, *Water Resources Research*, Vol. **32**, pp. 2135-2145.
- Band, L., E. and Moore, I., D. (1995): Scale: Landscape attributes and geographical information systems, *Scale Issues in Hydrological Modelling*, Kalma, J., D., Sivapalan, M. (eds), Wiley, Chichester, pp. 159-179.
- Beven, K., J. and Kirkby, M., J. (1979): A physically based, variable contributing area model of basin hydrology, *Hydrological Science Bulletin*, Vol. **24**, pp. 43-69.
- Beven, K. (1986): Runoff production and flood frequency in catchments of order n: An alternative approach, *Scale Problems in Hydrology*, Gupta, V., K., Rodríguez-Iturbe, I., Wood, E., F. (eds), Reidel Publishing Company, Dordrecht, pp. 107-131.
- Beven, K. (1987): Towards the use of catchment geomorphology in flood frequency predictions, *Earth Surface processes and Landforms*, Vol. **12**, pp. 69-82.
- Beven, K., J. (2000): *Rainfall-Runoff Modelling*, Wiley, New York.
- Beven, K., (2002): Towards an alternative blueprint for a physically based digitally simulated hydrologic response modeling system, *Hydrological Processes*, Vol. **16**, pp. 189-206.
- Bruneau, P., Gascuel-Oudou, C., Robin, P., Merot, Ph. and Beven, K., J. (1995): Sensitivity to space and time resolution of a hydrological model using digital elevation data, *Hydrological Processes*, Vol. **9**, pp. 69-82.
- Cunge, J., A. (1969): On the subject of a flood propagation computation method (Muskingum Method), *Journal of Hydraulic Research* Vol. **7**, pp. 205-230.

- Dunne, T. and Black, R., D. (1970): An experimental investigation of runoff production in permeable soils, *Water Resources Research*, Vol. **6**, pp. 478-490.
- Franchini, M., Wendling, J., Obled, Ch. and Todini, E. (1996): Some notes about the TOPMODEL sensitivity to basin topography, *Journal of Hydrology*, Vol. **175**: pp. 293-338.
- Freeze, R., A. and Harlan, R., L. (1969): Blueprint for a physically based, digitally simulated hydrological response model, *Journal of Hydrology*, Vol. **9**, pp. 237-258.
- Goodchild, M., F. (2001): Models of Scale and Scales of Modelling, *Modelling Scale in Geographical Information Science*, Tate, N., J. and Atkinson, P., M. (eds), Wiley, Chichester, pp. 3-10.
- Güntner, A., Uhlenbrook, S., Seibert, J. and Leibundgut, Ch. (1999): Multi-criterial validation of TOPMODEL in a mountainous catchment, *Hydrological Processes*, Vol. **13**, pp. 1603-1620.
- Iorgulescu, I. and Jordan, J-P. (1994): Validation of TOPMODEL on a small Swiss catchment, *Journal of Hydrology*, Vol. **159**: pp. 255-273.
- Jenson, S., K. and Domingue, J., Q. (1988): Extracting Topographic Structures from Digital Elevation Data for Geographic Information Systems Analysis, *Photogrammetric Engineering and Remote Sensing*, Vol. **54**, pp. 1593-1600.
- Kirkby, M., J. (1975): Hydrograph modeling strategies, *Process in Physical and Human Geography*, Peel, R., Chisholm, M., Haggett, P. (eds), Heinemann, London, pp. 69-90.
- Klinkenberg, B. and Goodchild, M., F. (1992): The fractal properties of topography: a comparison of methods, *Earth Surface processes and Landforms*, Vol. **17**, pp. 217-234.
- Martz, L., W. and Garbrecht, J. (1992): Numerical Definition of Drainage Network and Subcatchment Areas from Digital Elevation Models, *Computers and Geosciences*, Vol. **18**, pp. 747-761.
- Mendicino, G. and Sole, A. (1997): The information content theory for the estimation of the topographic index distribution used in TOPMODEL, *Hydrological Processes*, Vol. **11**, pp. 1099-1114.
- O'Callaghan, J., F. and Mark, D., M. (1984): The extraction of drainage networks from Digital Elevation Data, *Computer Vision, Graphics and Image Processing*, Vol. **28**, pp. 323-344.
- Pradhan, N., R. and Jha, R. (2003): Performance assessment of BTOPMC model in a Nepalese drainage basin, *Weather radar information and distributed hydrological modeling*, Tachikawa, Y., Vieux, B., E., Georgakakos, K., P., Nakakita, E. (eds), IAHS Publication No. 282, pp. 288-293.
- Pradhan, N., R., Tachikawa, Y. and Takara, K. (2004): A scale invariance model for spatial downscaling of topographic index in TOPMODEL, *Annual Journal of Hydraulic Engineering, JSCE*, Vol. **48**, pp. 109-114.
- Quinn, P., Beven, K., Chevallier, P. and Planchon, O. (1991): The prediction of hillslope flow paths for distributed hydrological modeling using digital terrain models, *Hydrological Processes*, Vol. **5**, pp. 59-79.
- Rogers, C., C., M., Beven, K., J., Morris, E., M. and Anderson, M., G. (1985): Sensitivity Analysis, Calibration and Predictive Uncertainty of Institute of Hydrology Distributed Model, *Journal of Hydrology*, Vol. **81**: pp. 179-187.
- Saulnier, G-M., Obled, Ch. and Beven, K., J. (1997): Analytical compensation between DTM grid resolution and effective values of saturated hydraulic conductivity within the TOPMODEL framework, *Hydrological Processes*, Vol. **11**, pp. 1131-1144.
- Wolock, D., M. and Price, C., V. (1994): Effects of digital elevation model map scale and data resolution on a topography based watershed model,

- Water Resources Research*, Vol. **30**, pp. 3041-3052.
- Zhang, W. and Montgomery, D., R. (1994): Digital elevation model grid size, landscape representation, and hydrologic simulations, *Water Resources Research*, Vol. **30**, pp. 1019-1028.
- Zhang, X., Drake, N., A., Wainwright, J. and Mulligan, M. (1999): Comparison of slope estimates from low resolution DEMs: Scaling issues and a fractal method for their solution, *Earth Surface Processes and Landforms*, Vol. **24**, pp. 763-779.

スケールに依存しない物理的水文モデル:スケール不変 TOPMODEL の開発

ナワ, ラジャ, プラダン*・立川康人・寶 馨

*京都大学大学院工学研究科土木工学専攻

要 旨

粗い分解能の数値標高データを用いてTOPMODELの地形指標分布を求めると、実際の地形が有する地形情報が失われてしまう。この欠点を補うために、本研究ではリゾリューションファクターとフラクタルとを用いて、等高線単位長さ当りの上流面積と勾配に対するスケール効果を取り除く手法を提案する。この手法を用いることにより、粗い分解能を持つ数値標高データを用いた場合も、詳細な標高データを用いた場合と同等の地形指標分布を得ることが可能となる。このダウンスケールされた地形指標をTOPMODELに組み込むことにより、スケール不変TOPMODELを開発する。上椎葉ダム流域(210 km²)に本手法を適用し、1000m分解能の標高データから得られる地形指標分布と50m分解能の標高データから得られる地形指標分布とが極めてよく一致することを確認した。また、50m分解能のTOPMODELを用いて同定されるモデルパラメータを、1000m分解能の標高データからダウンスケールして得られるスケール不変TOPMODELに組み込んだところ、ダウンスケールされたスケール不変TOPMODELモデルによる流出計算結果と50m分解能TOPMODELモデルの流出計算結果とが極めてよく一致した。これによりスケール不変TOPMODELを用いることによって、ある空間スケールのTOPMODELモデルによって得られたパラメータ値が、異なる空間スケールのモデルでも利用可能であることを示した。

キーワード: スケール不変, ダウンスケール, フラクタル, 地形指標, TOPMODEL